Non-Monotonicity of p_T correlations at RHIC

Rutik Manikandhan (University of Houston)
for the STAR Collaboration

Supported in part by U.S. DEPARTMENT OF ENERGY

Phase Diagram of Nuclear Matter

- Two distinct phases of matter confirmed
- Crossover at low μ_B ($\mu_B/T < 2$)
- Predictions of 1st order phase transition at high μ_B
- Where is the transition line at high density?
- Is there a Critical End Point (CEP) ?

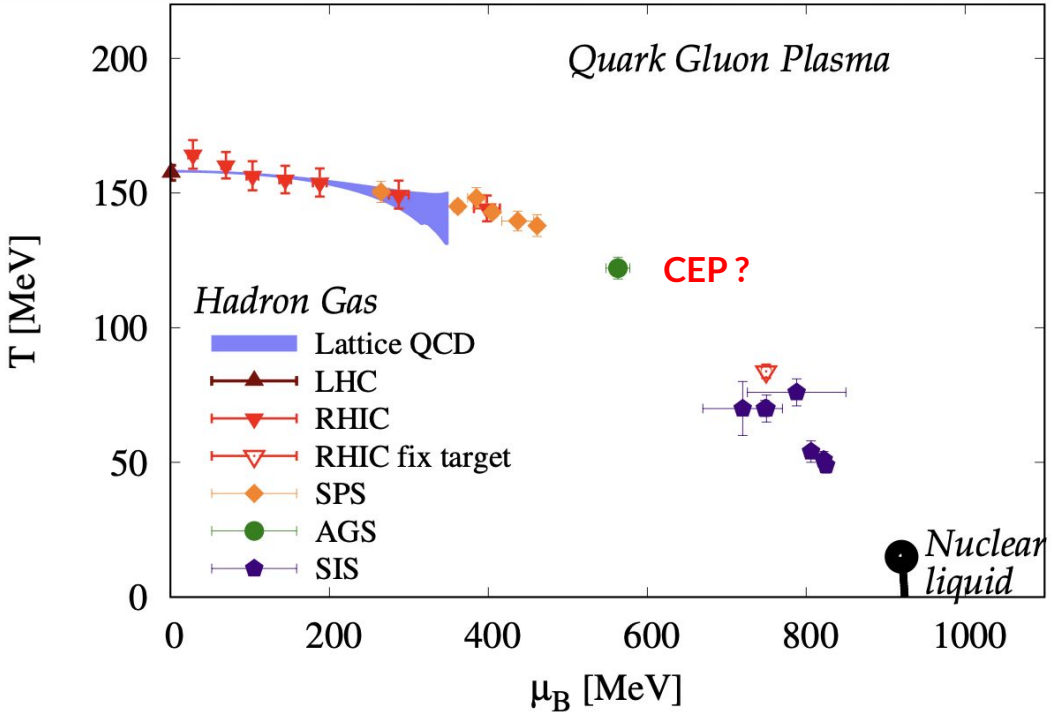

S. Borsanyi et. al. : https://arxiv.org/abs/2512.08843

Search for the Critical End Point (CEP)

- A wide array of non-perturbative frameworks (Lattice QCD, DSE, FRG, and Holography) provide diverse predictions for the CEP coordinates in the (T, μ_B) plane.
- Modern functional methods and refined models show a strong convergence of predicted points within the 3–6 GeV energy range.
- The STAR experiment is currently the only experimental facility capable of accessing this high-density regime.

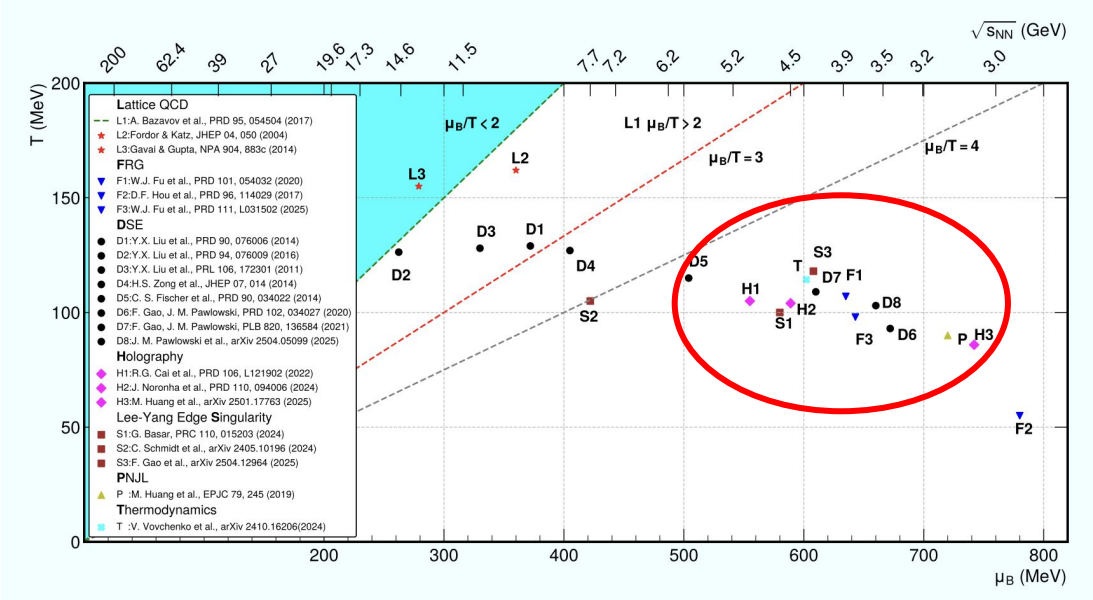

Eluding us for many years!

Y. Zhang et. al. : arXiv:2602.08356

Probe for the QCD phase diagram

- In high-energy nuclear collisions, early hard scatterings generate initial partonic correlations governed by QCD.

S. Gavin : Phys. Rev. Lett. 92, (2003)

- Transverse momentum $\langle p_T \rangle$ correlators measure pairwise momentum correlations and probe these early dynamics.

$$C_m = < \Delta p_{t,i} , \Delta p_{t,j} >$$

$$< (p_{t,i} - < p_t >)(p_{t,j} - < p_t >) >$$

$$i \neq j$$

- They are sensitive to the QCD critical point, where enhanced fluctuations and long-range correlations are expected.

M . Stephanov et. al. : Phys. Rev. Lett. 81, (1998)

- Measured correlators include contributions from both early partonic interactions and later hadronic final-state effects.

Probe for the QCD phase diagram

- Multiparticle $\langle p_T \rangle$ correlators are sensitive only to dynamical fluctuations and therefore provide a direct measure of the correlations of interest.
- This feature makes $\langle p_T \rangle$ correlations robust against volume fluctuations and insensitive to the details of the centrality selection.
- Final measurement is quoted as the scaled correlator $C_{pT} \sim v_0(\text{int})$

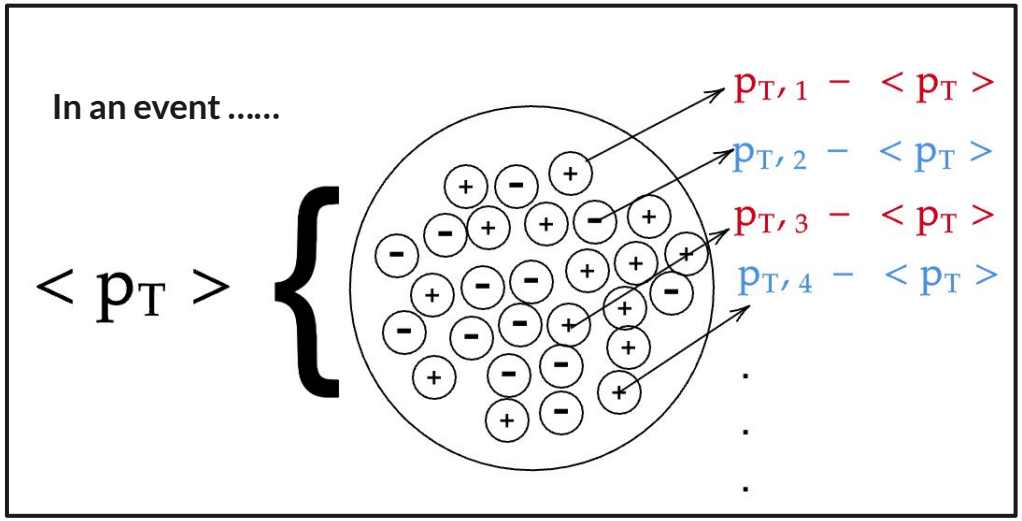

$$C_{p_T} = \frac{\sqrt{\langle \Delta p_{T,i} \Delta p_{T,j} \rangle}}{\langle \langle p_T \rangle \rangle}$$

B. Schenke et. al. : Phys. Rev. C 102, (2020)

Why study $\langle p_T \rangle$ correlations in HIC?

- Correlators have contributions from dynamic correlations from the first partons produced.
- These correlations get erased by scattering and thermalization.
- The rapid expansion and short lifetime of the system fight the forces of isotropization, preventing certain correlations from being completely thermalized.
- Inclusive observable sensitive to multiple physics sources:
  - Conserved charge fluctuations
  - Temperature fluctuations

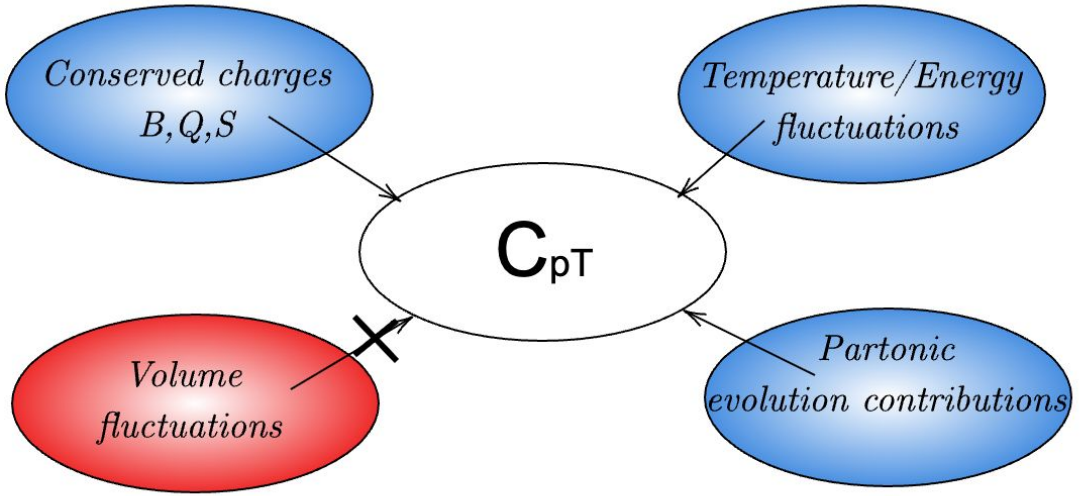

Oleh Savchuk : J. Phys. G: Nucl. Part. Phys. 52 (2025)

S. Pratt et. al. : Phys. Rev. C 104 (2021)

Kitazawa et. al. : YITP-25-161, J-PARC-TH (2025)

BES-I Scan at RHIC

- Two-particle correlations measured and compared to CERES and ALICE measurements.
- A monotonous collision energy dependence was found for $\langle p_T \rangle$ correlations.
- Important for measurements from BES-II FXT regime to probe critical phenomena.

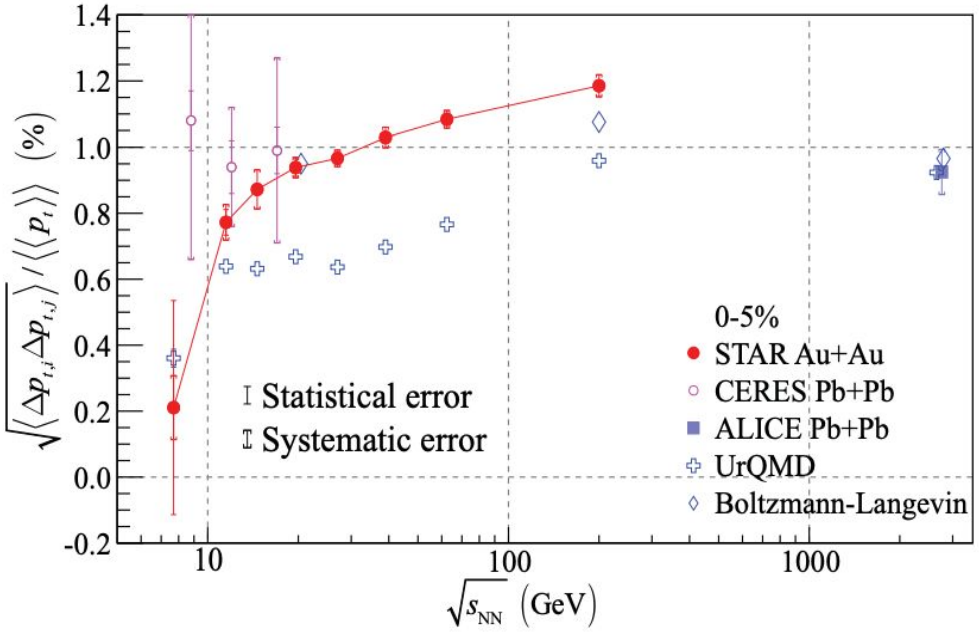

STAR : Phys. Rev. C 99, (2019)
CERES : Nucl.Phys.A811 (2008)
ALICE : Eur. Phys. J. C 74 (2014)

$$7.7 \lesssim \sqrt{s_{NN}}\text{(GeV)} \lesssim 200 \rightarrow 420 \gtrsim \mu_B\text{(MeV)} \gtrsim 25$$

BES-II Scan at RHIC

- High precision data
- Wide μ_B coverage: Probing QCD phase diagram upto 760 MeV
- Increased statistics for 7.7 GeV (Collider) by a factor of 50.
- Unique cross-check of Collider vs. Fixed-Target (FXT) correspondence.

$\sqrt{s_{NN}}$(GeV)	No. of Events collected (10^6)	μ_B(MeV)
3.0 (FXT)	260+2000	760
3.2 (FXT)	200	699
3.5 (FXT)	120	670
3.9 (FXT)	120	633
4.5 (FXT)	110	590
5.2 (FXT)	100	540
7.7 (FXT)	260	420
7.7 (COL)	104	420

$$3 \lesssim \sqrt{s_{NN}}\text{(GeV)} \lesssim 7.7 \rightarrow 760 \gtrsim \mu_B\text{(MeV)} \gtrsim 420$$

A. Lysenko et. al. : Phys. Rev. C 111 (2025)

Kinematic Acceptances

- Only TPC used for analysis

  Z. Sweger et. al. : Phys. Rev. C 111, (2025)
- Common acceptance window across the entire BES energies
- Slight loss at 7.7 GeV fixed-target, 7.7 GeV center-of-mass complements and verifies results.
- Intense cross checks performed to verify consistency between FXT ad COL measurements.
- Dashed blue line shows mid-pseudo-rapidity
- Solid black box shows acceptance window

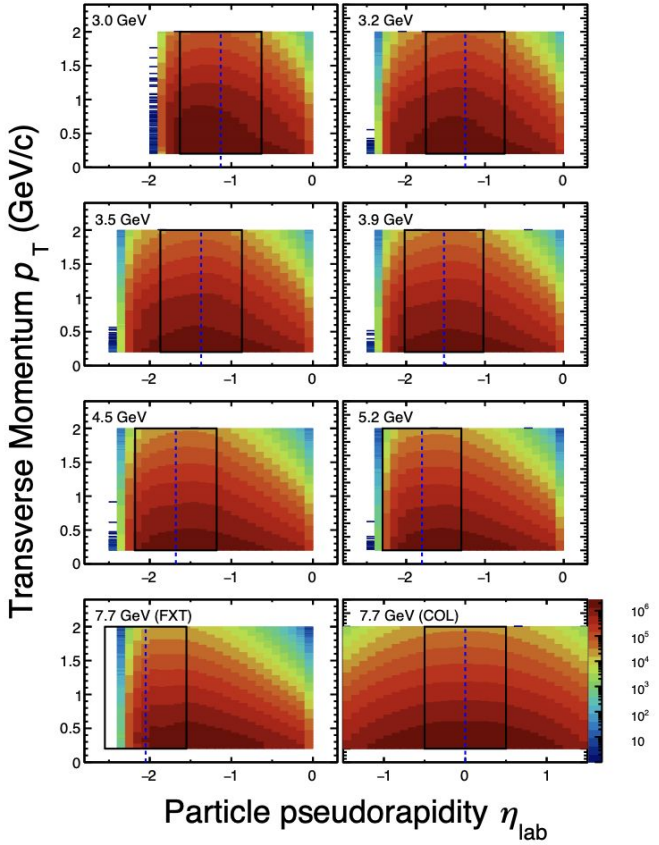

Event-by-Event $\langle p_T \rangle$ Distributions

- Raw $\langle p_T \rangle$ distributions from BES-II, uncorrected for detector efficiency
- **Mean increases for with decreasing collision energy: Effect of Baryon stopping**
- **Width increases for decreasing collision energy: Effect of decreased particle production**
- Gamma function distributions explain the data *M. Tannenbaum: Phys.Lett.B 498 (2001)*

$$\Gamma(\alpha,\beta) = \frac{x^{\alpha-1} e^{\frac{-x}{\beta}}}{\Gamma(\alpha)\beta^{\alpha}}$$

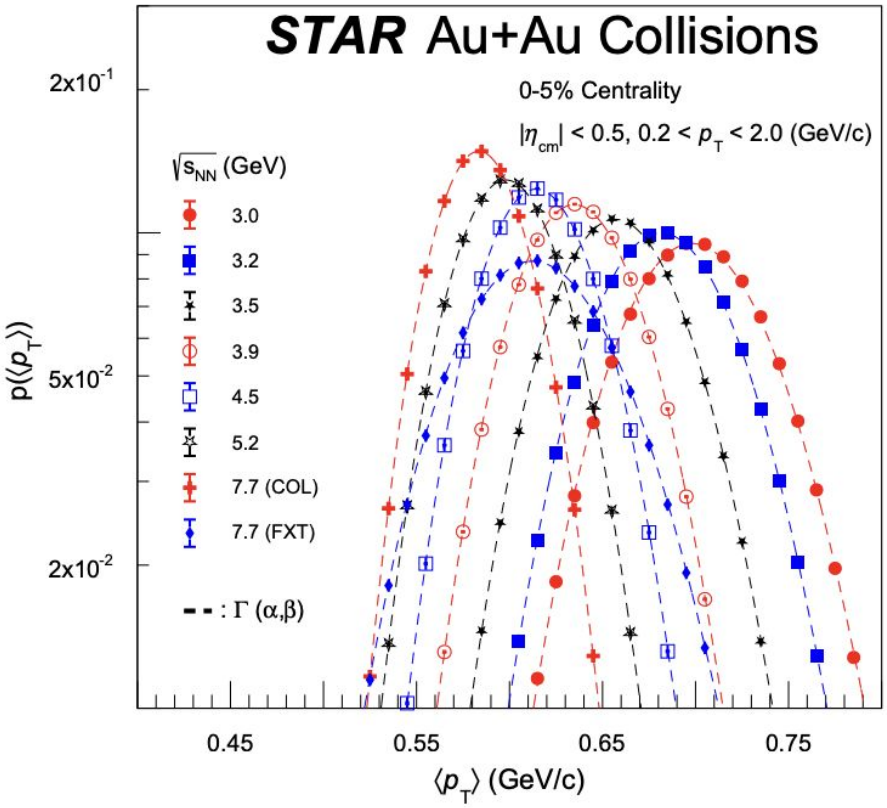

Discrepancy @ 7.7 GeV (COL & FXT) ?

- $\langle p_T \rangle$ distributions at $\sqrt{s_{NN}}$ = 7.7 GeV differ between collider and FXT modes due to acceptance effects.
- $\langle p_T \rangle$ is an extensive observable and is therefore sensitive to particle loss and phase-space coverage.
- The scaled correlator is an intensive observable, making it largely insensitive to acceptance differences.

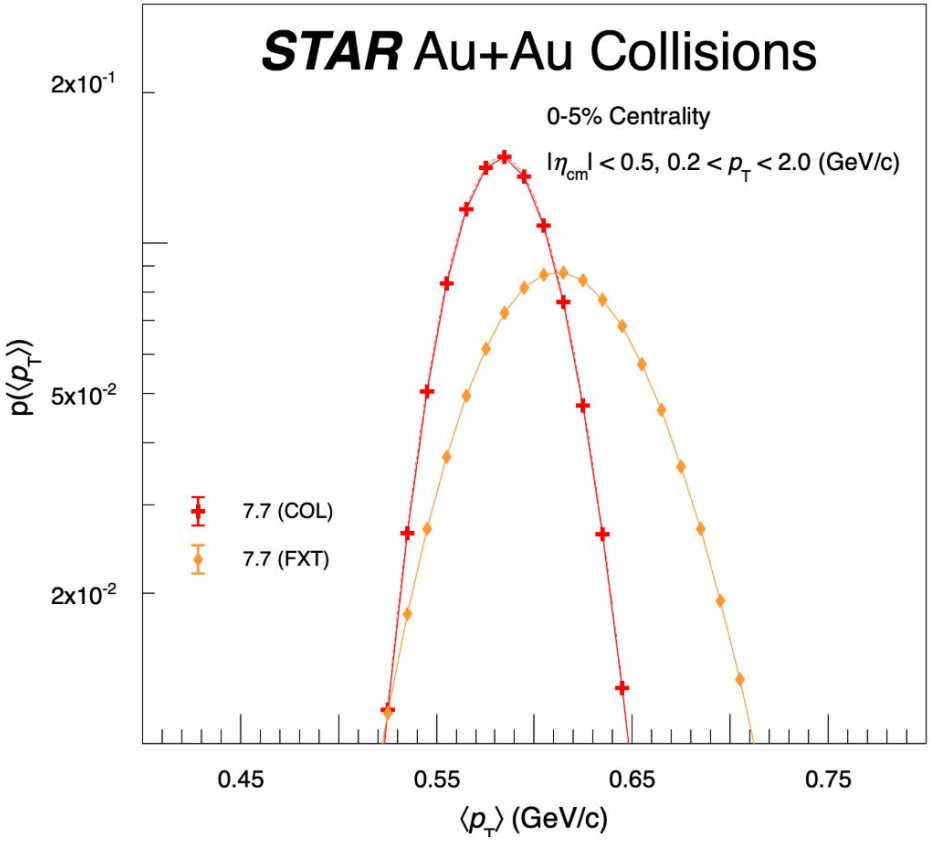

UrQMD Study

- Before applying acceptance and efficiency losses, the distributions are identical for both modes.
- After applying acceptance and efficiency effects, the FXT mode exhibits broader distributions and a shift in the mean, consistent with observations in data.
- Note: UrQMD is used only to qualitatively understand the impact of acceptance and efficiency; a one-to-one correspondence between data and UrQMD is not expected

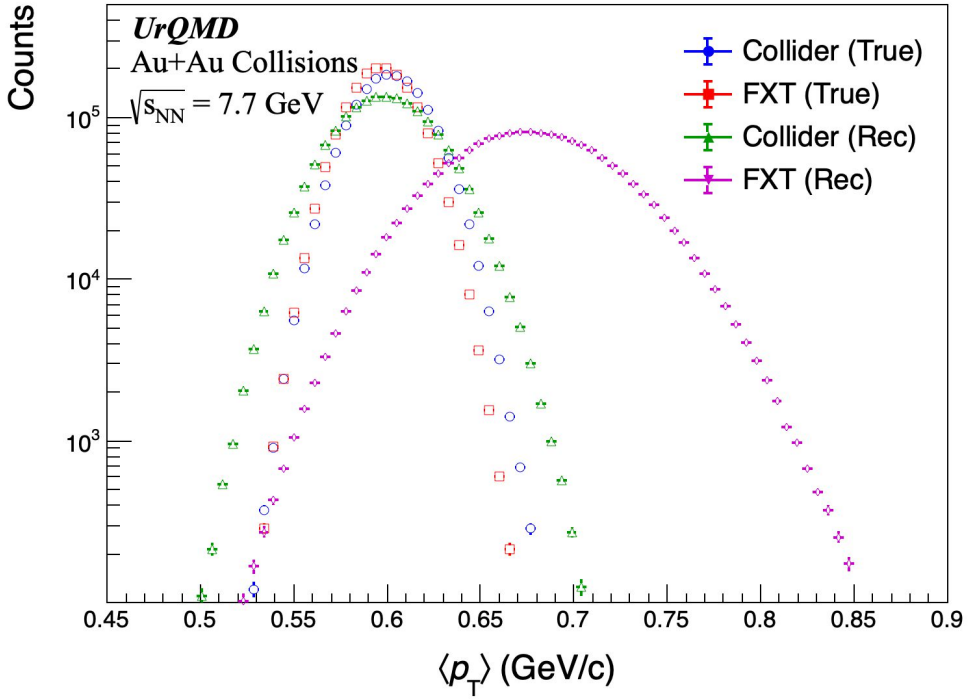

Consistency @ 7.7 GeV (FXT & COL)

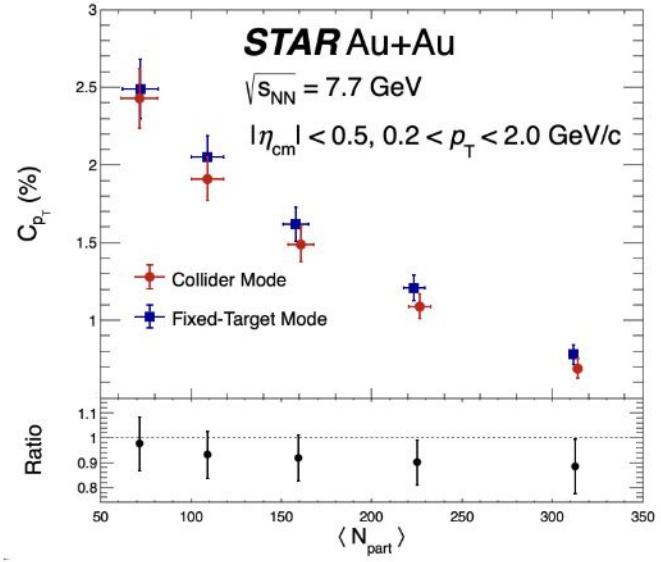

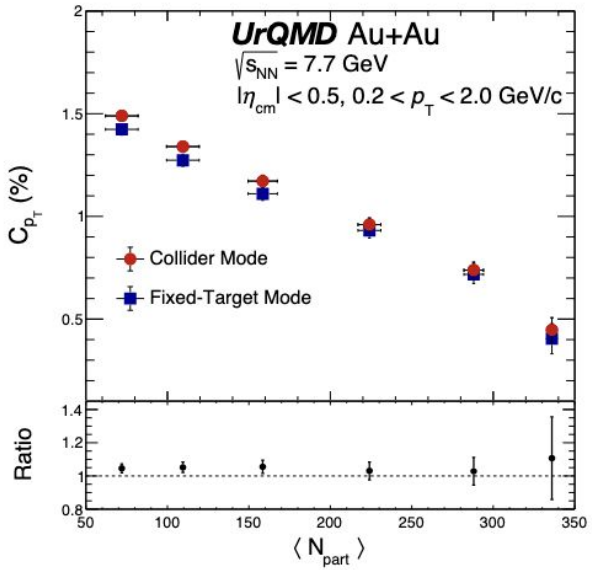

- We see consistency between the modes in STAR data and within our model study.
- The intensive nature of the variable ensures this consistency.
- Observable is independent of acceptance and efficiency losses.
- First observation of consistency between two different modes

Volume fluctuations

- Initial volume fluctuations (IVF) due to lack of centrality resolution
- Huge concern at lower BES-II energies
- Shown to affect proton cumulants significantly
- Centrality Bin Width correction does not fully correct it
- IVF can mask the true signal

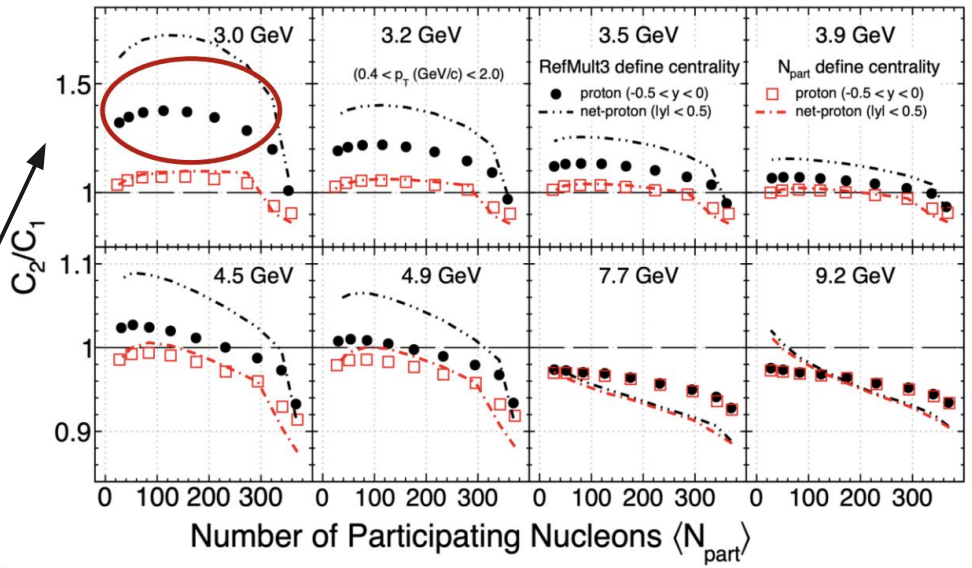

Xin Zhang et. al. : 2026 Chinese Phys. C 50 011003

Effect of Volume fluctuations on C_{pT}

- Cross-check the effect of centrality bin width correction (CBWC) at $\sqrt{s_{NN}}$ = 7.7 GeV
- CBWC: compute observables in each multiplicity bin, then perform event-weighted averaging within a centrality class (e.g., 0–5%).
  X. Luo et. al. : *J. Phys. G: Nucl. Part. Phys.* 40 105104
- Removes residual dependence on centrality-bin width for extensive quantities.
- **C_{pT} is independent of CBWC and bin size, consistent with its intensive nature.**

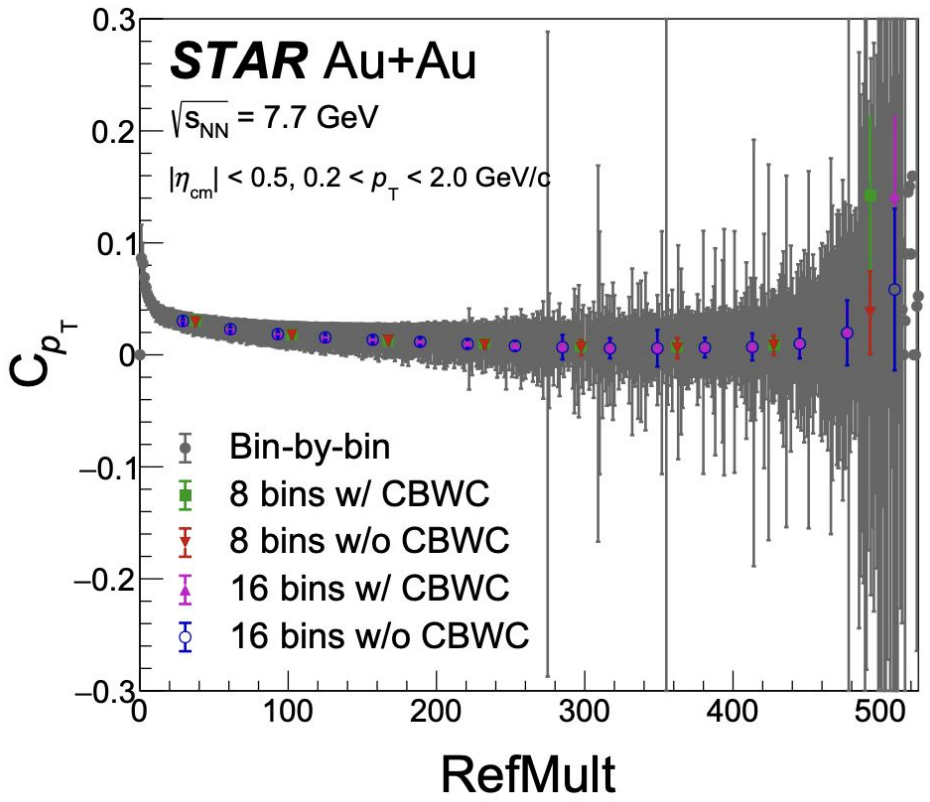

Centrality Dependence of C_{pT}

- Most sources of $\langle p_T \rangle$ fluctuations are stochastic, encompassing fluctuations in nucleon and parton positions within the initial state and temperature fluctuations of QGP fluid cells.

  P. Biozek, et. al. : Phys. Rev. C 85, (2012)

- Hence, cumulants of $\langle p_T \rangle$ are anticipated to scale inversely with the number of participating nucleons (Npart) in a simple power-law manner,

- Namely:

  - $\langle (\delta \langle p_T \rangle)^2 \rangle \propto 1/N_{part}$
  - $\langle (\delta \langle p_T \rangle)^3 \rangle \propto 1/N^2_{part}$

  M. Cody et. al. : Phys. Rev. C 107, (2023)

- This scaling limit is referred to as the independent source model scenario.

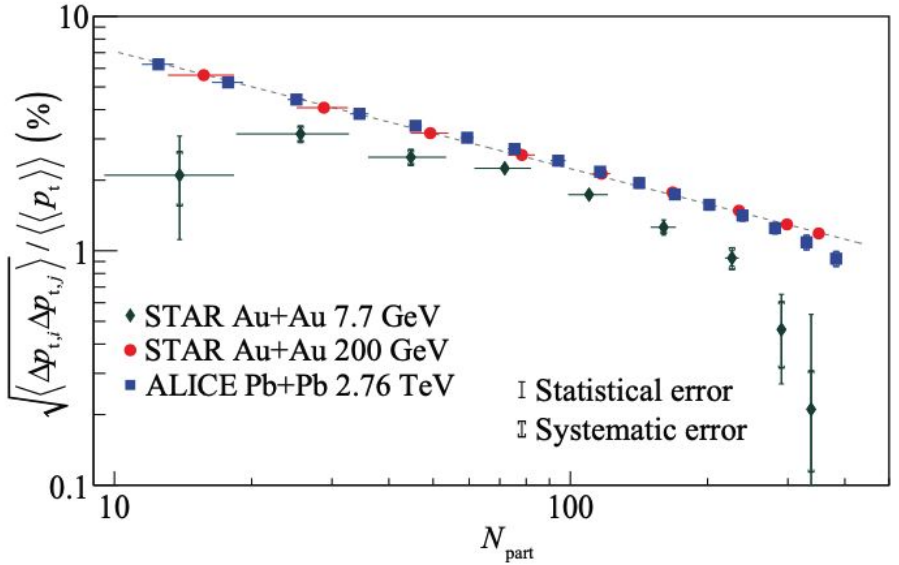

ISM: $C_{p_T} \propto \langle N_{part} \rangle^{-0.5}$

Centrality Dependence of C_{pT} (BES-II)

- Due to limited multiplicity at low energies, the exponent is fixed to the expected baseline value of −0.5 (not a free parameter).
- This differs from LHC analyses (ALICE, ATLAS), where the exponent is fitted freely thanks to higher statistics. *ALICE* : Eur. Phys. J. C 74 (2014) *ATLAS:* Phys. Rev. Lett. 133, (2024)
- **We observe at 3.0 GeV breakdown of this scaling, possibly due to dominance of hadronic interactions.**
- **The deviations in 0-10% suggest the onset of additional dynamical effects beyond trivial statistical fluctuations.** *S. Gavin :* Phys. Rev. Lett. 92, (2003)

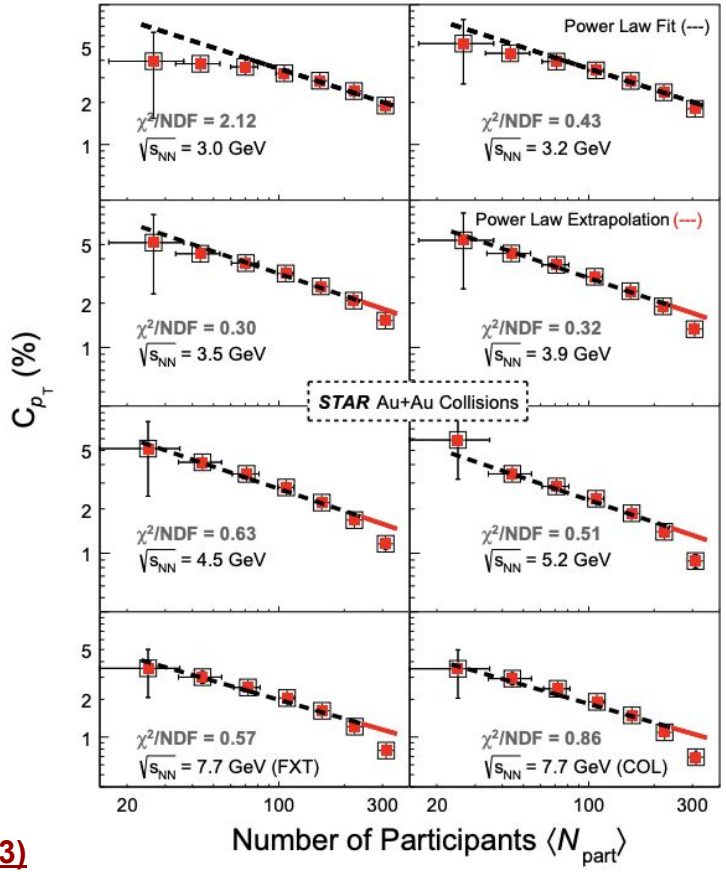

Centrality Dependence of C_{pT} (BES-I,II)

- BES-I results are published
  STAR : Phys. Rev. C 99, (2019)
- Each collision energy has their own scaling
- Obtained deviation from respective ISM scaling
- **Observed largest deviation in $\sqrt{s_{NN}}$ = 5.2 - 11.5 GeV region**

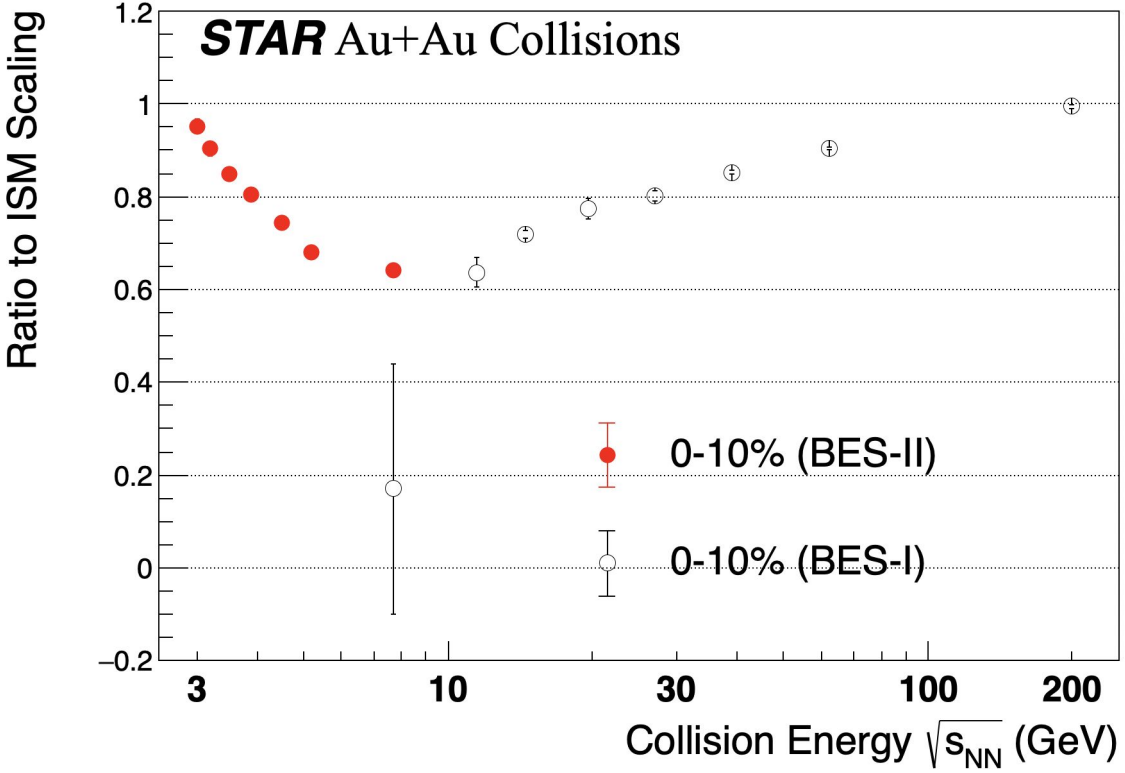

Energy dependence of C_{pT}

- BES-I results show a monotonic dependence on collision energy.
- The trend is stronger in central (0–5%) than mid-central (30–40%) collisions.
- The Boltzmann–Langevin model reproduces the observed behavior.

S. Gavin et. al. : Phys. Rev. C 95, (2017)

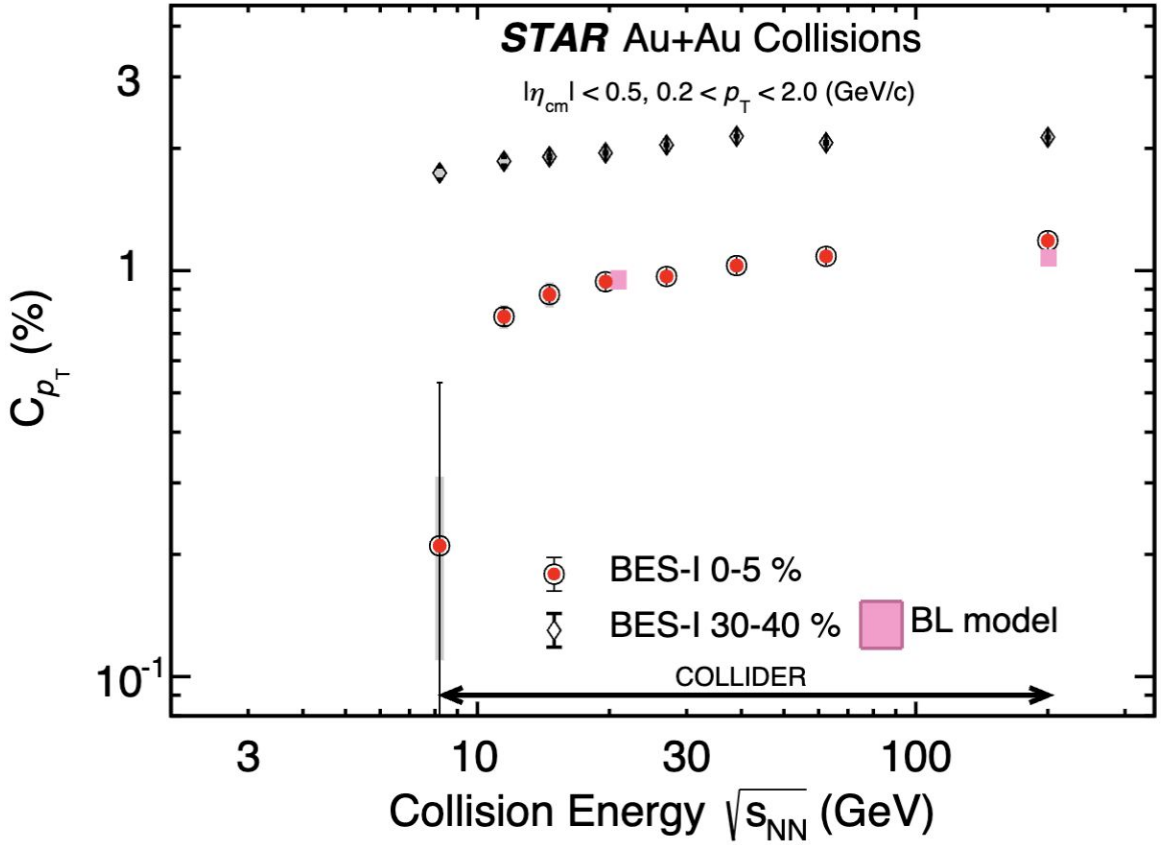

Energy dependence of C_{pT}

- BES-I results show a monotonic dependence on collision energy.
- The trend is stronger in central (0–5%) than mid-central (30–40%) collisions.
- The Boltzmann–Langevin model reproduces the observed behavior.
  S. Gavin et. al. : Phys. Rev. C 95, (2017)
- **BES-II results show a significant non-monotonic behavior in 0–5% central collisions, but not in 30–40%.**
- At 7.7 GeV, BES-II is consistent with BES-I, with substantially reduced uncertainties.

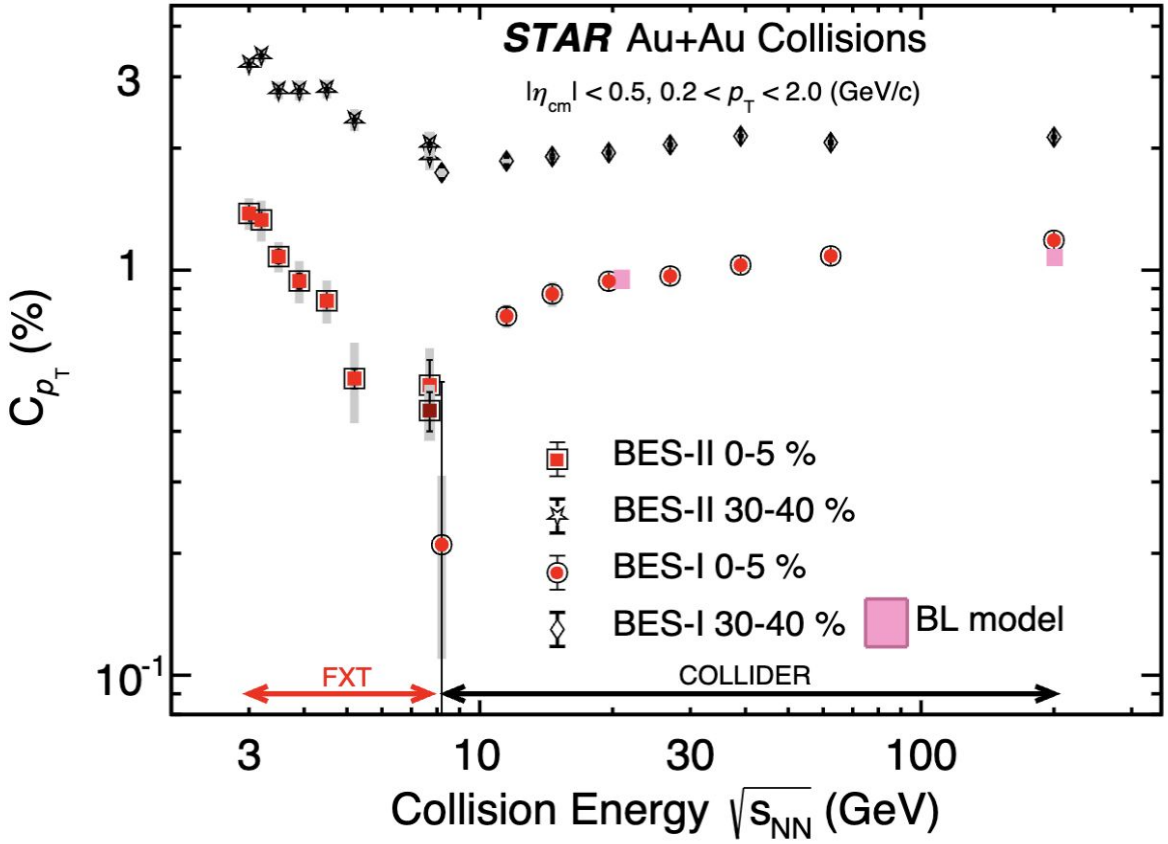

Energy dependence of C_{pT}

- BES-I results show a monotonic dependence on collision energy.
- The trend is stronger in central (0–5%) than mid-central (30–40%) collisions.
- The Boltzmann–Langevin model reproduces the observed behavior.
  S. Gavin et. al. : Phys. Rev. C 95, (2017)
- **BES-II results show a significant non-monotonic behavior in 0–5% central collisions, but not in 30–40%.**
- At 7.7 GeV, BES-II is consistent with BES-I, with substantially reduced uncertainties.
- AMPT describes mid-central (30–40%) data, but cannot reproduce the central (0–5%) behavior.
  L. Zhang et. al. : Phys. Rev. C 111, (2025)

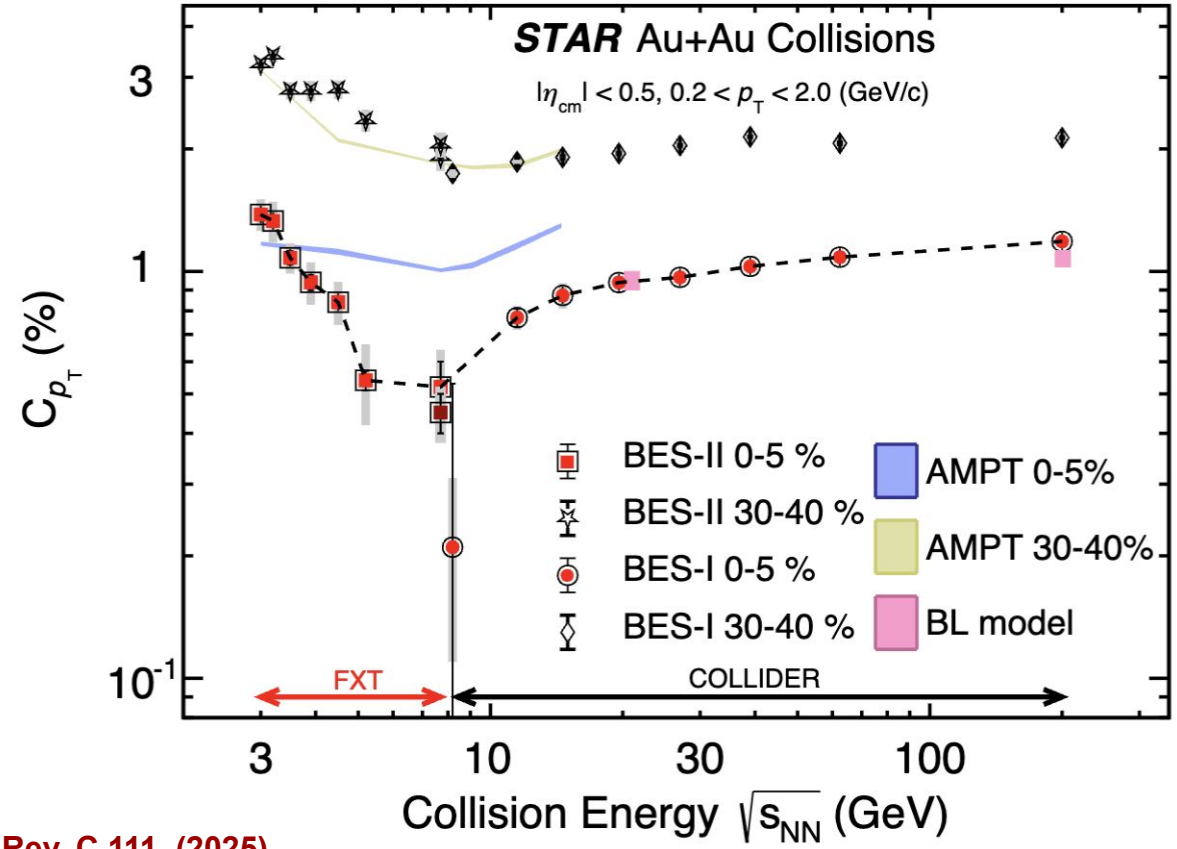

Quantifying Non-Monotonicity

- Quantify non-monotonicity by fitting the energy dependence with a strictly monotonic reference (first-order polynomial).
- Anchor the fit to high-energy points with the smallest uncertainties to define a data-driven baseline.
- Minimize model bias and avoid overfitting statistical fluctuations.

STAR 0-5 %	~5.5 σ
AMPT 0-5 %	~1.4 σ
STAR 30-40 %	~2 σ

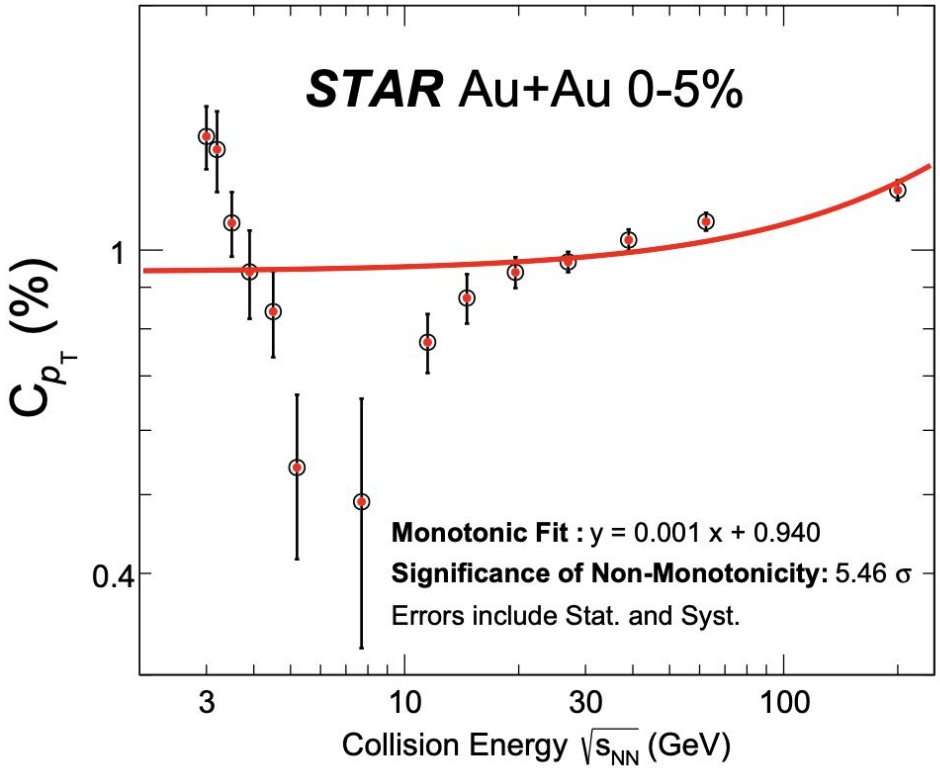

Quantifying Non-Monotonicity

- Alternate method was proposed to quantify non-monotonicity
- Ratio was constructed between 0-5% and 30-40%
- Fit to a monotonous function
- Obtained ~5 σ significance of non-monotonicity
- Non-monotonic significance confirmed using two methods

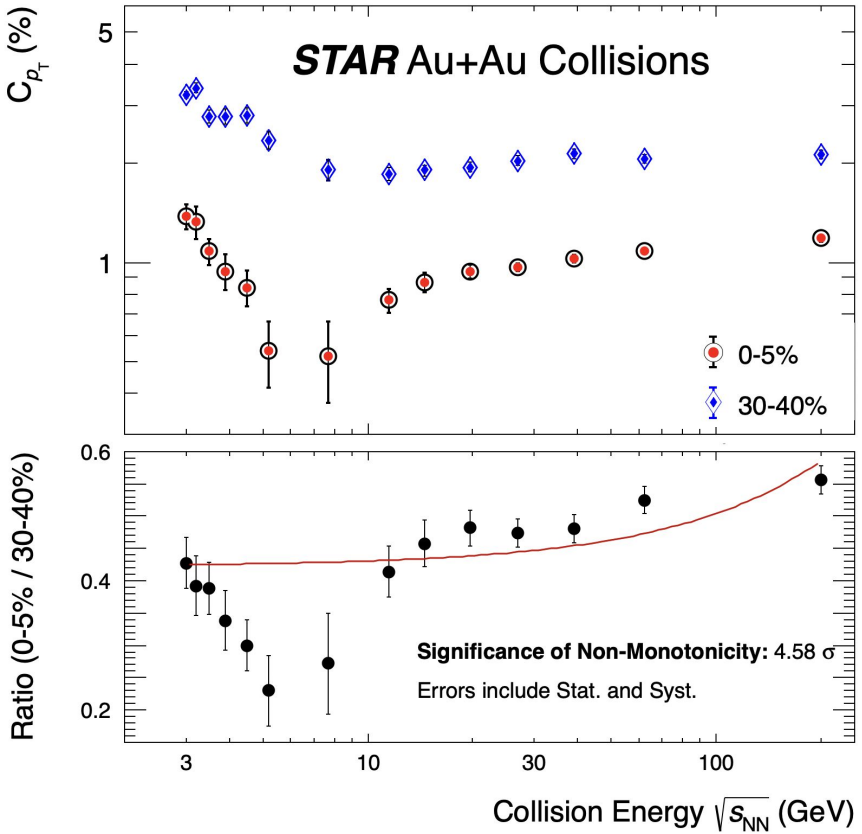

Conclusions

- First observation of non-monotonic behavior in $\langle p_T \rangle$ correlations in most central collisions
- The observed dip aligns with the predicted location of the critical point across multiple theoretical models.
- We observe maximum deviation in $\sqrt{s_{NN}}$ = 5 - 8 GeV region
  ➢ μ_B ~ 600 - 400 MeV
- First observation of breakdown of Independent sources scaling at $\sqrt{s_{NN}}$ = 3.0 GeV

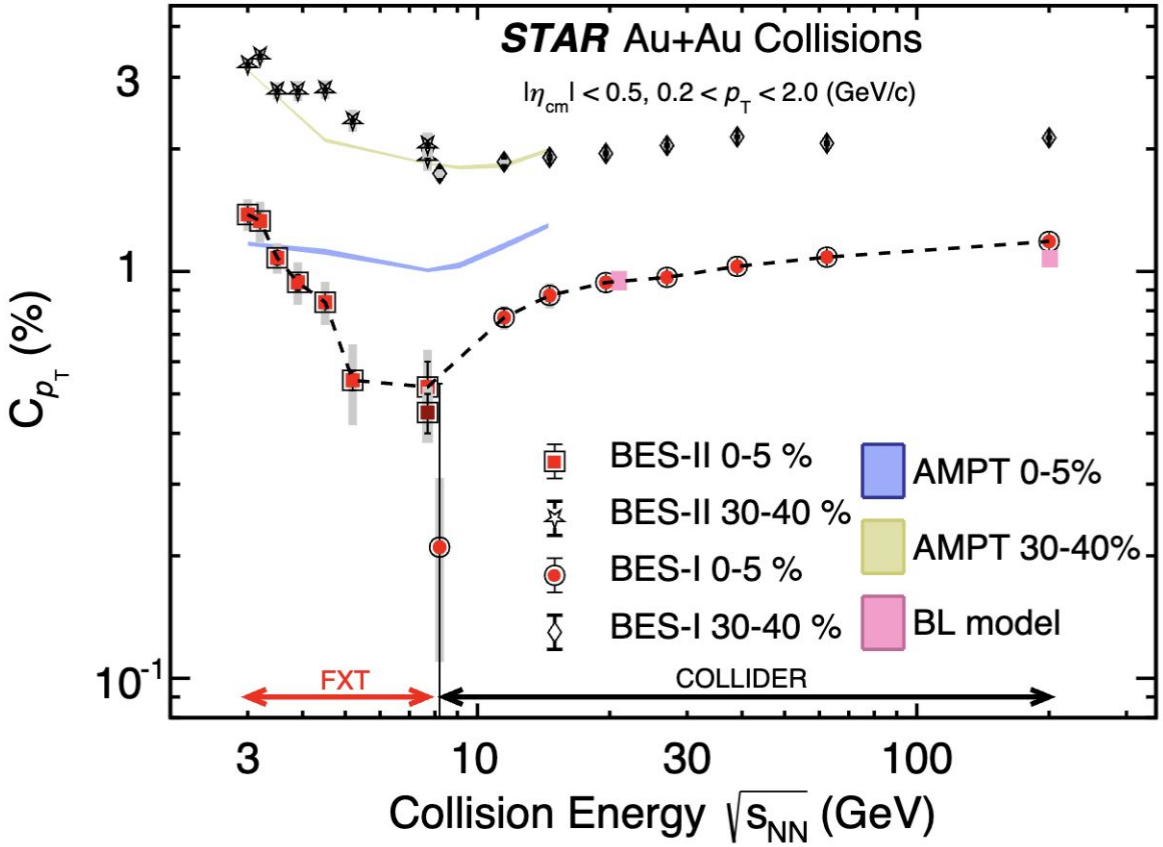

Backup

Partial Thermalization

- Scattering among these partons leads to dissipation that works to erase these correlations, making the system as thermal and locally isotropic as possible.
- The rapid expansion and short lifetime of the system fight the forces of isotropization, preventing certain correlations from being completely thermalized.

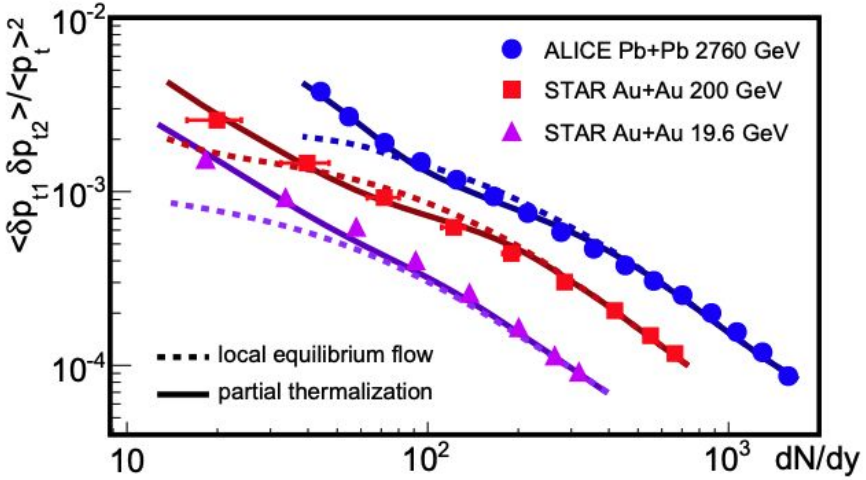

FIG. 1. (color online) Transverse momentum fluctuations as a function of the charged-particle rapidity density dN/dy for partial thermalization (solid curves) and local equilibrium flow (dashed curves). Data (circles, squares, and triangles) are from Refs. [27], [31], and [32, 33], respectively.

Comparison of Centrality Dependences

R. Manikandhan et. al. (in preparation)

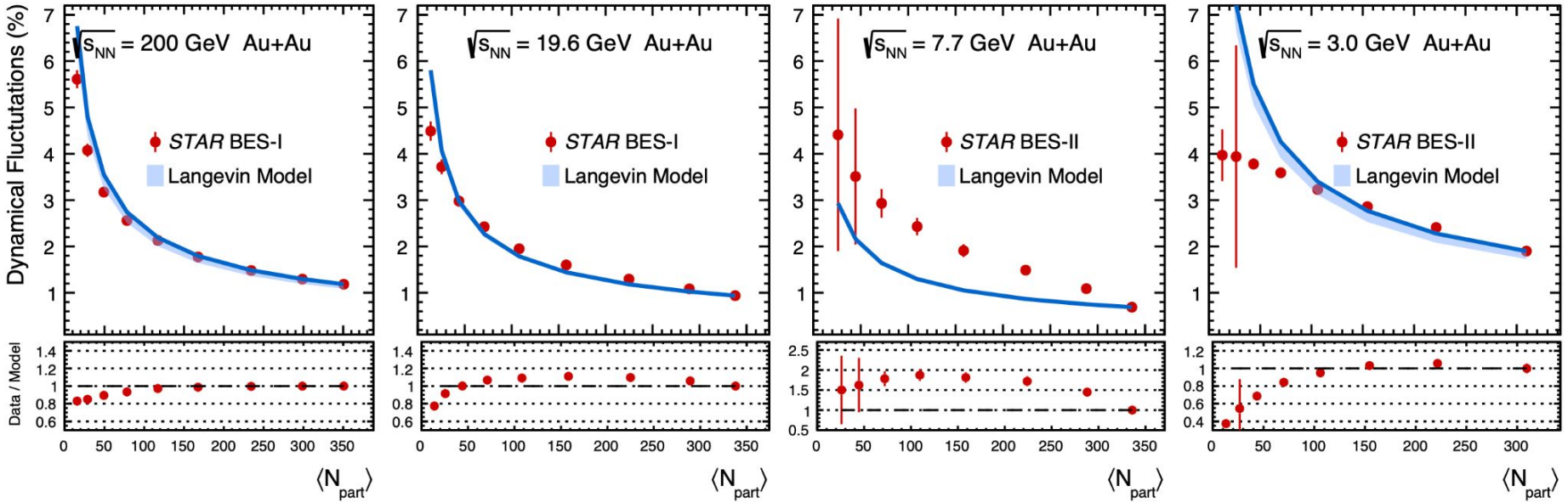

- We normalize to the most central bin, to study centrality dependence.
- The area of overlap A(⟨N_{part}⟩) is feeded to the viscosity term.
- We capture the data at $\sqrt{s_{NN}}$ 200 -19.6 GeV
- Significant deviations around $\sqrt{s_{NN}}$ 7.7 -3 GeV

Comparison of Collision Energy Dependence

- First unified baseline spanning the full BES range
- First lattice QCD–constrained EoS implemented in dynamical fluctuation p_T correlator
- Transport models (AMPT) are limited in energy coverage and rely on different mechanisms across $\sqrt{s_{NN}}$, lacking a common QCD-based thermodynamic foundation
- Predicts a smooth, monotonic energy dependence in the absence of critical effects
- Establishes a consistent QCD-grounded reference for isolating genuine critical signatures

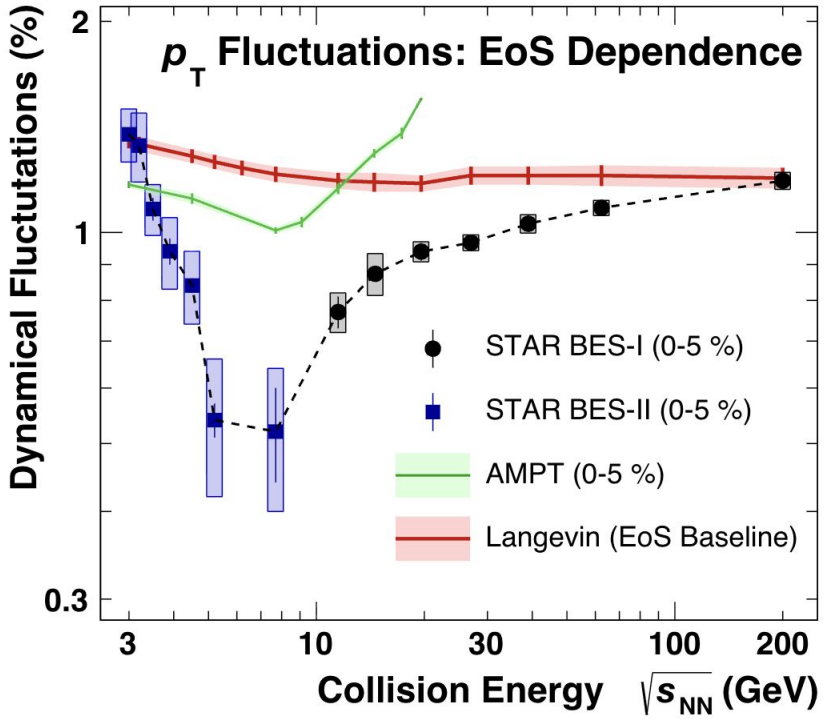

R. Manikandhan et. al. (in preparation)

Correlator Vs Acceptance

1. We change the window size around mid rapidity at all energies.

2. $\Delta\eta$ = 2.0
   a. full TPC (FXT mode) acceptance [-2,0]

3. $\Delta\eta$ = 0.4
   a. +/- 0.2 around midrapidity

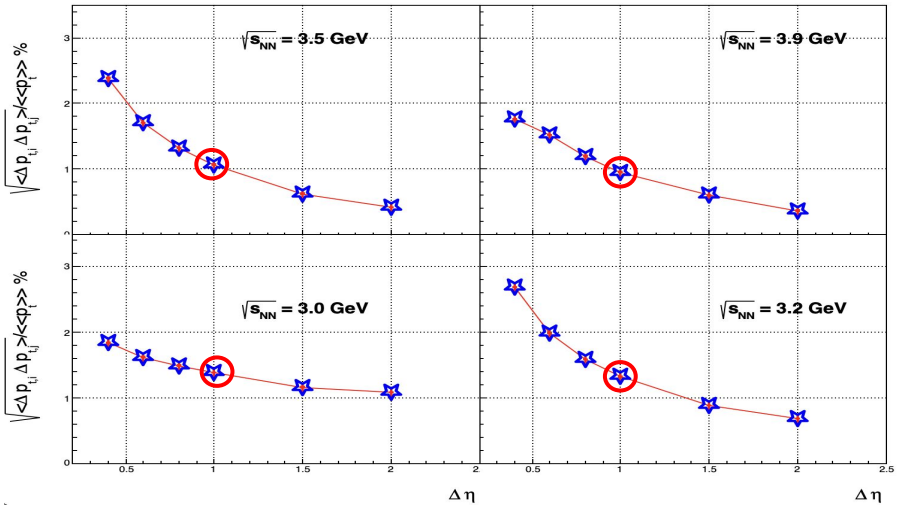

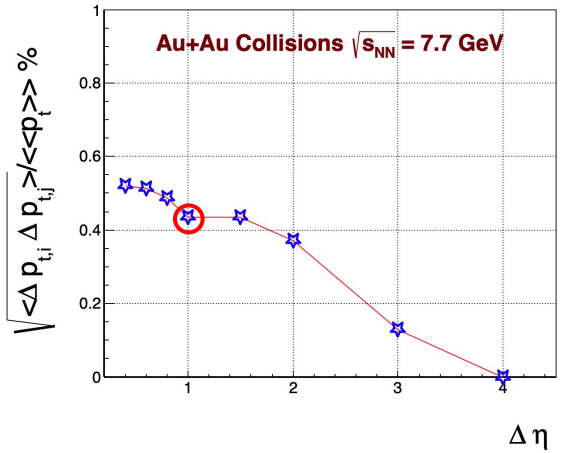

STAR-FXT

- **STAR** Detector
- Particle Identification
  - TPC ($-2.0 < \eta_{lab} < 0$)
  - w iTPC ($-2.2 < \eta_{lab} < 0$)
  - TOF ($-1.5 < \eta_{lab} < 0$)
- Possible dependence of efficiency in different pseudorapidity regions ??

Solenoidal Tracker At RHIC

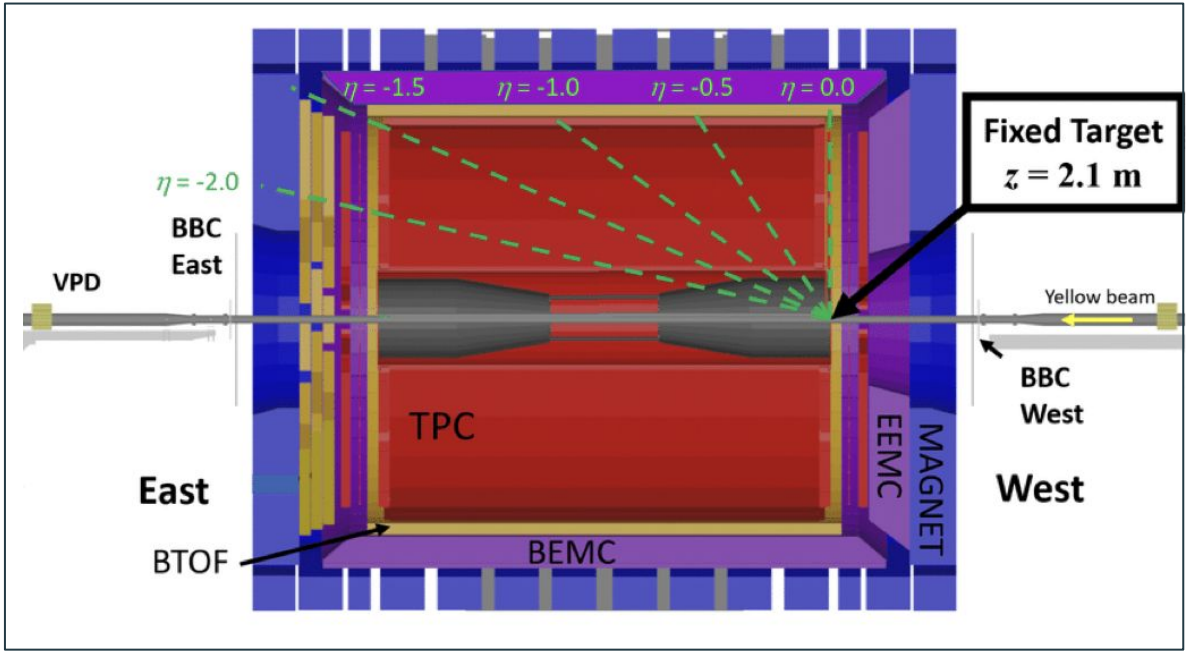

www.star.bnl.gov

UrQMD with Phase transitions

CMF-PT1 and PT2 refer to first-order phase transitions at 2.5 and 4 times saturation density, respectively

https://arxiv.org/abs/2208.12091

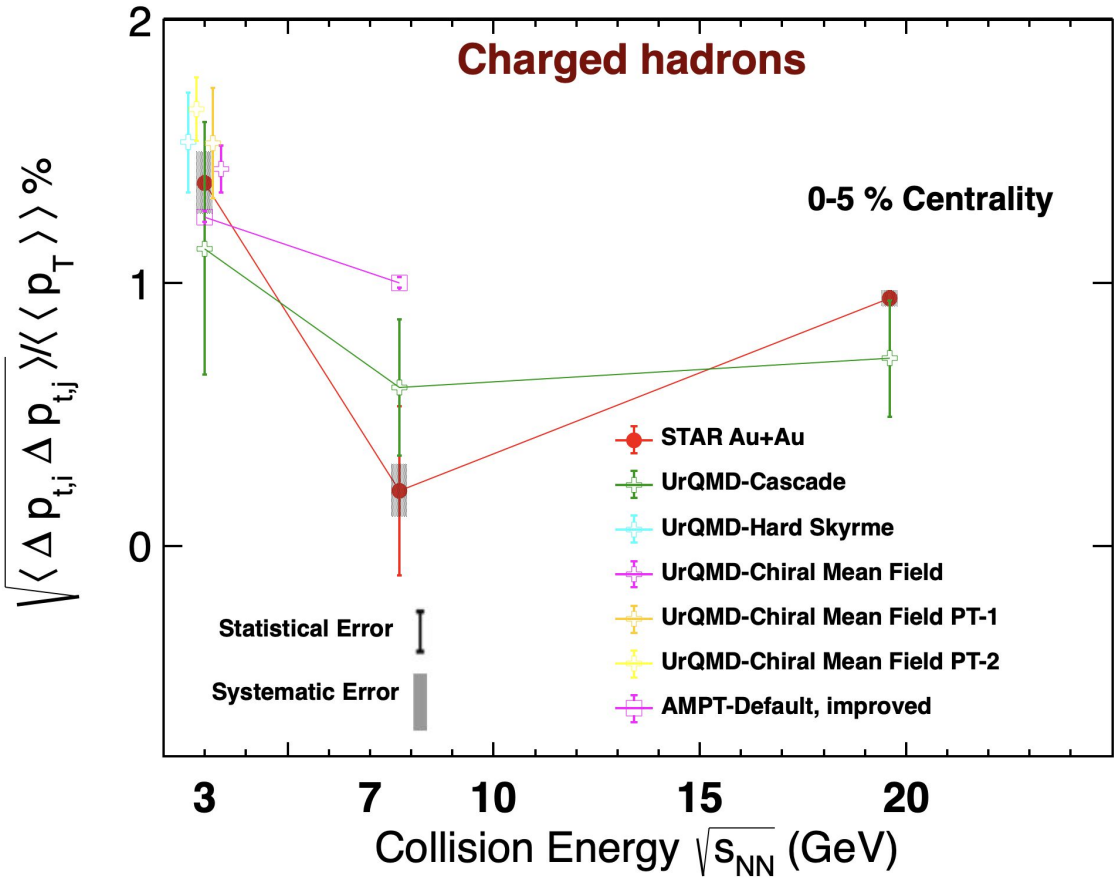

Correlator Vs Collision Energy

Diagnostic plots

Pion p_T-p_T Correlators,

1. if p<0.55 (GeV/c)
   a. $|n_\sigma \text{pions}| < 2$
   b. $|n_\sigma \text{others}| > 2$
2. if p>0.55 (GeV/c)
   a. $|n_\sigma \text{pions TOF}| < 3$
   b. $-0.05 < m^2 < 0.08$
   c. $|1/\beta - 1/\beta_\pi| < 0.015$
3. DCA < 3 cm
4. Blue side very few particles.

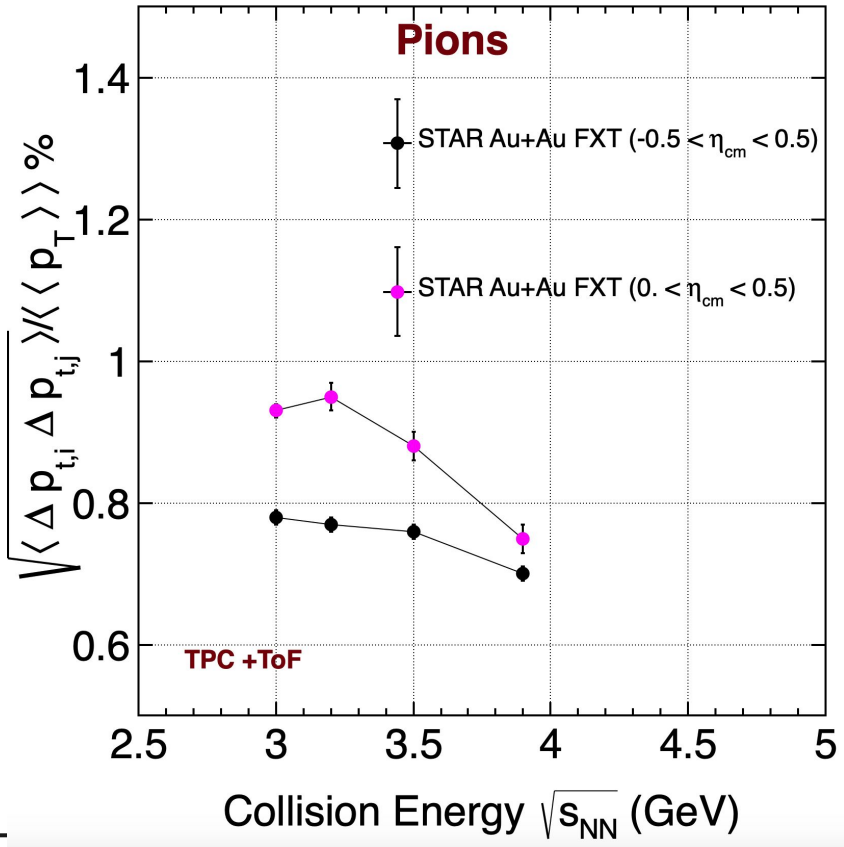

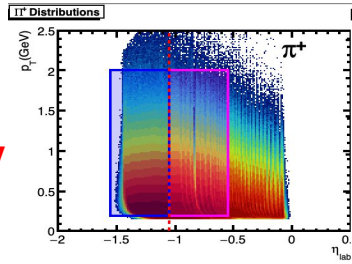

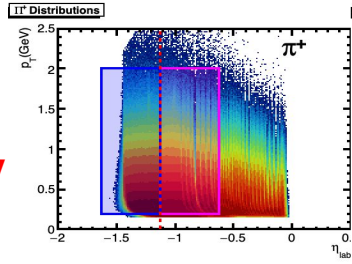

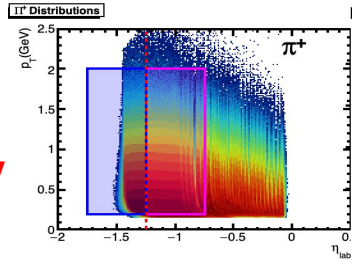

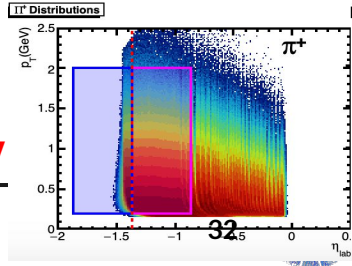

Correlator Vs Collision Energy

Diagnostic plots

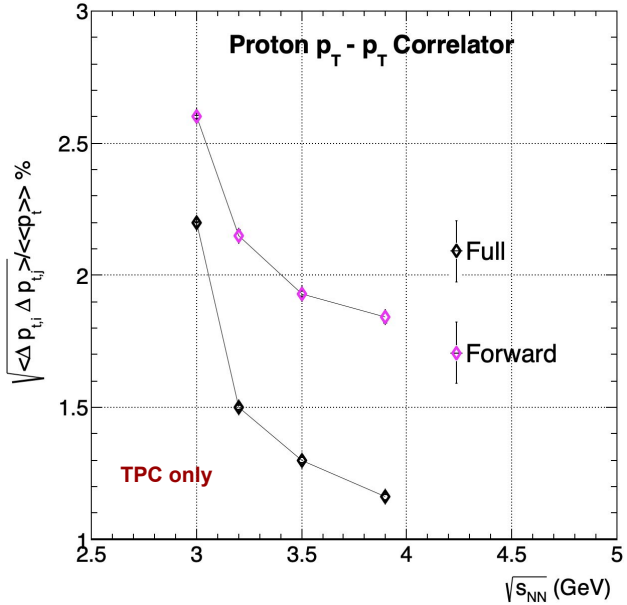

Protons identified using TPC only:

1. $|n_{\sigma}^{protons}| < 2$
2. DCA < 2 cm
3. $|n_{\sigma}^{others}| > 2$

Auto Correlation Studies

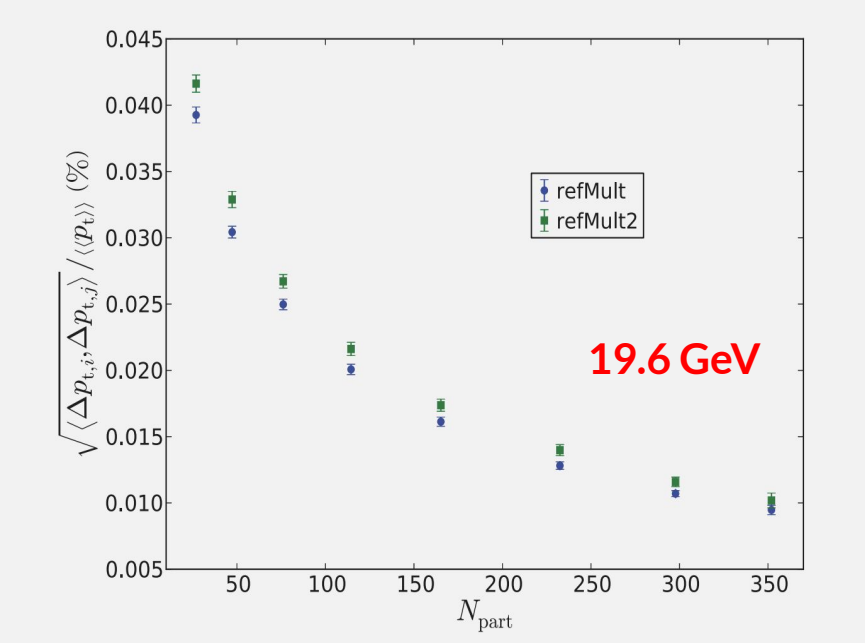

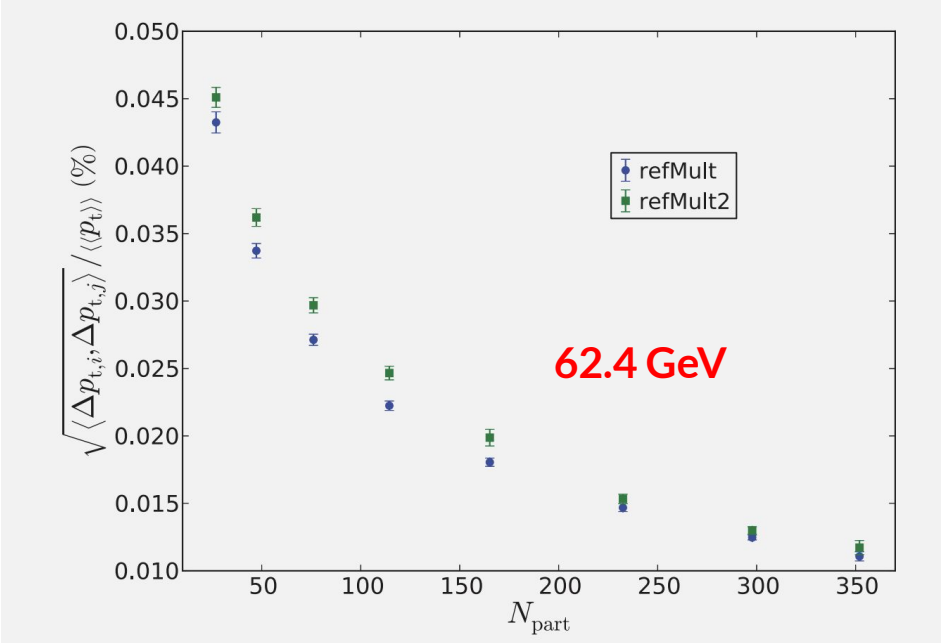

https://groups.nscl.msu.edu/nscl_library/Thesis/Novak,%20John.pdf

T_{chem} Vs μ_B

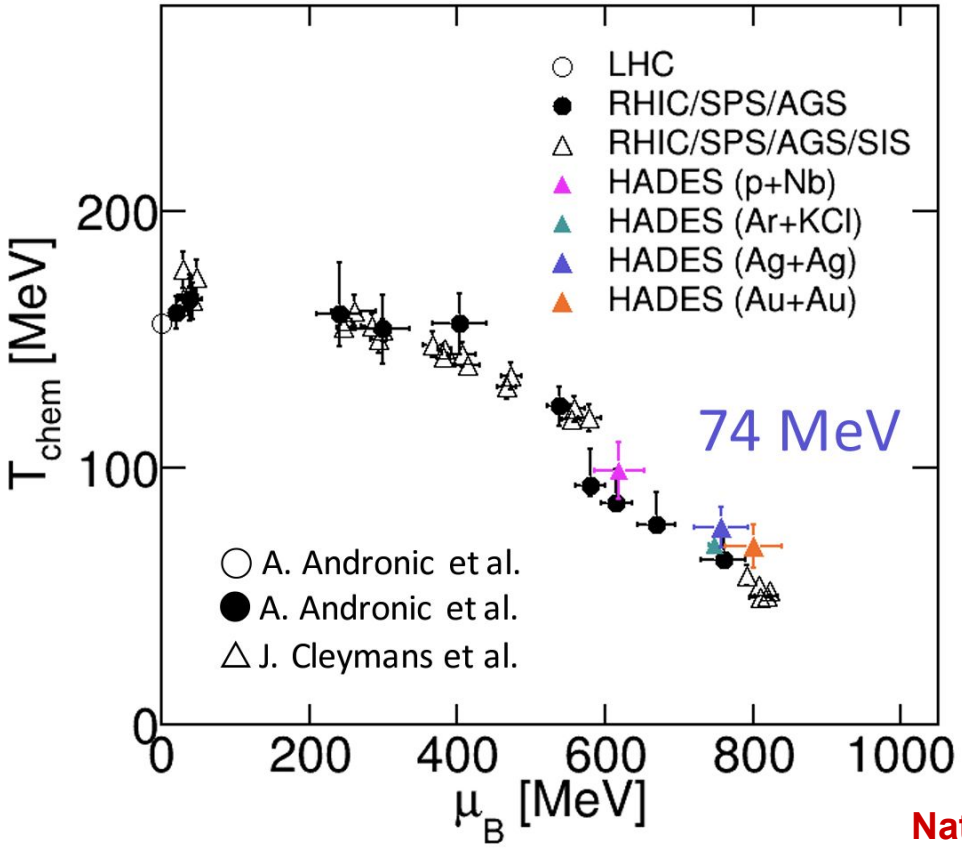

Nature Phys. 15 (2019) 10, 1040-1045

Contributions to temperature fluctuations

$$\sigma^2_{T_{eff}} \approx \sigma^2_{T_{kin}} + m_0^2\sigma^2_{\langle\beta_T\rangle^2}$$

$$+ 2m_0 \mathrm{Cov}\left(T_{kin}, \langle\beta_T\rangle^2\right)$$

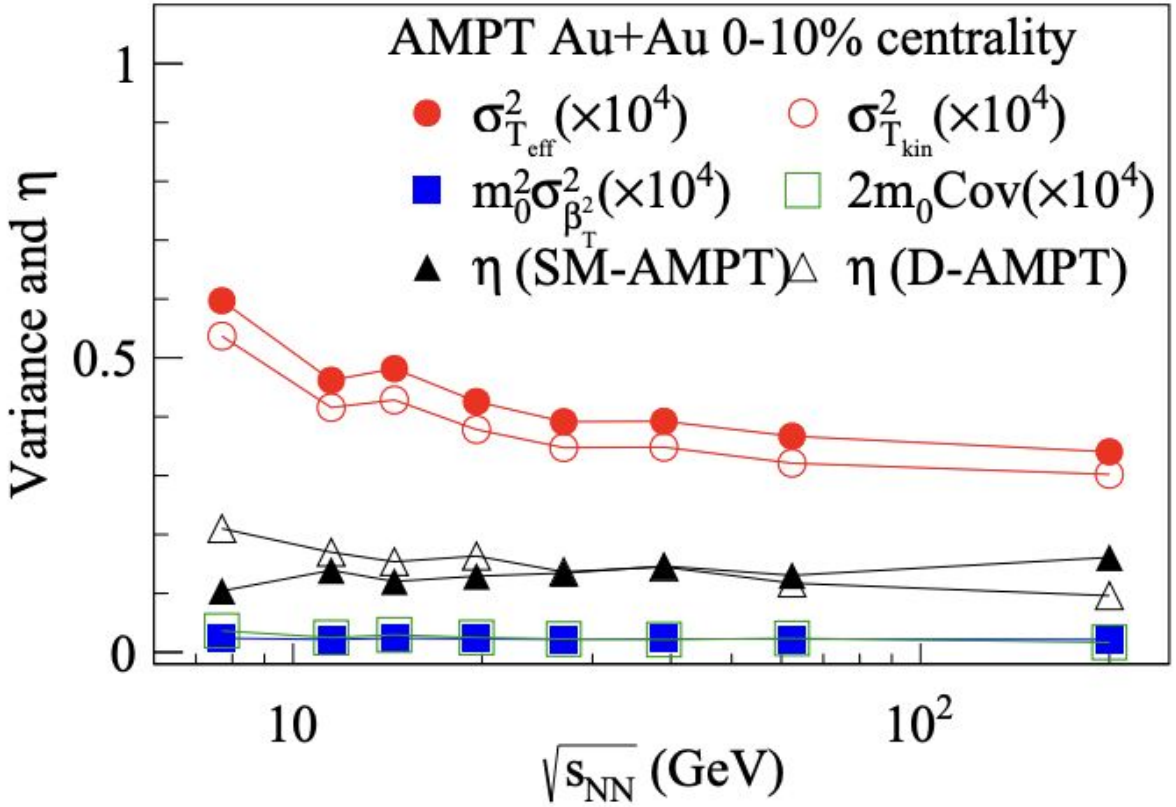

Phys.Rev.C 106 (2022) 1, 014910